INDICATIONS OF NEUTRINO OSCILLATION IN THE K2K NEUTRINO OSCILLATION EXPERIMENT

Taku Ishida, representing K2K collaboration
Institute for Particle and Nuclear Studies(IPNS)
High Energy Accelerator Research Organization(KEK)
1-1 Oho, Tsukuba-shi, Ibaraki 305-0801, Japan

Abstract

The indications of neutrino oscillation observed by the K2K long-baseline neutrino oscillation experiment are presented in this talk: From 1999 to 2001, 5.6×10^{19} protons on target were delivered to the experiment in 234.8 days of running. During this period there were 56 events fully contained in the Super-Kamiokande inner detector fiducial area, which was synchronized to the beam-spill timing. In the case of no oscillations, the expected number of events was $80.1^{+6.2}_{-5.4}$. Out of the 56 events, we obtained 29 events of single ring μ-like events. The neutrino energy spectrum for the events, reconstructed by assuming two-body kinematics of quasi-elastic interactions, shows a deficit in the E_ν=0.5$\sim$1GeV bin, compared with the spectrum at the production observed by the near detectors. These two facts indicate neutrino oscillation with common oscillation parameter regions. A combined oscillation analysis gives $\Delta m^2 = 1.5 \sim 3.9 \times 10^{-3}\mathrm{eV}^2$ at $sin^2 2\theta$=1.0 at the 90% confidence level, and the null oscillation probability is found to be less than 1%.

1 Introduction

The atmospheric neutrino anomaly observed by Super-Kamiokande(SK) and other recent underground experiments strongly suggest $\nu_\mu \leftrightarrow \nu_\tau$ neutrino oscillation. The allowed region of the oscillation parameters are in the range of $\Delta m^2_{atm} = 1.6 \sim 3.9 \times 10^{-3}$ eV^2 and $sin^2 2\theta_{atm} > 0.92$ at the 90% confidence level, [2] where Δm^2_{atm} is the mass-difference squared between two neutrino mass eigenstates and θ_{atm} is the mixing angle between two neutrinos. The principal goal of the K2K (*KEK-to-Kamioka*) experiment is to confirm neutrino oscillation with a man-made neutrino beam and to measure the oscillation parameters. We use the 12-GeV PS at KEK as a neutrino source, which produces a wide-band neutrino beam with an average energy of $\overline{E}_\nu$=1.3 GeV. The far detector, Super-Kamiokande, a 50 kt water Cherenkov detector, is located L =250km East from KEK. In order to measure the effects of oscillation we compare the total number of events and the ν_μ spectrum observed by SK to those expected from measurements by a near detector system at KEK. A deficit of ν_μ events and / or a distortion of the neutrino spectrum are evidence of neutrino oscillation. Owing to the E_ν/L value, which is in a similar range to that of atmospheric neutrinos, we have sensitivity to explore a similar mass-difference region, $\Delta m^2 \geq 2 \times 10^{-3}$eV^2.

2 The K2K experiment

Fig. 1 shows a bird's-eye view of the neutrino beam-line at KEK. The 12-GeV PS provides $\sim 6 \times 10^{12}$ protons per spill every 2.2 sec, and each spill has 9 bunches in a 1.1 μsec spill width. Protons are bent in the direction of Kamioka in the primary beam line, and are injected on aluminum target of 3cm$\phi \times 66cm$ length, embedded in the 1^{st} horn magnet. Two horn magnets [3] focus the produced positively-charged pions effectively towards the direction of Kamioka. The neutrino beam strength becomes $\times \sim 20$ larger than in the case without them. The produced pions decay into μ and ν_μ within 200m of a decay pipe filled with helium gas, and the produced ν_μ beam flys underground to the SK direction with a tilting angle of -1°. The neutrino flux and the spectrum shape at SK is expected to be the same within 3$m$rad, because the neutrino beam divergence is mainly determined by the decay kinematics of the pions. We measure the profile of muons from pion decays by ionization chambers and silicon pad detectors located behind the beam dump, which indirectly guarantees that the center of the neutrino beam profile is stable *spill-by-spill* within $\leq \pm 1m$rad. A pion monitoring gas Cherenkov counter [4] is occasionally placed in the beam axis downstream of the 2^{nd} horn. By adjusting the internal gas pressure, it can explore the momentum and angle distribution of the produced pions in $p_\pi \geq$2GeV/c, without suffering any effect from the

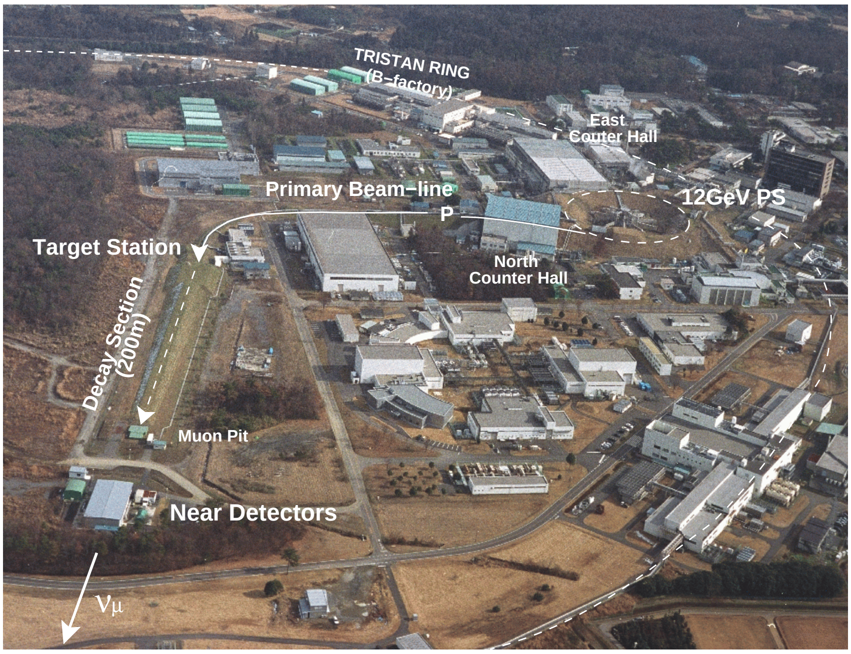

Figure 1: *Bird's-eye view of the neutrino beam-line at KEK. Each beam-line component is explained in the main text. A near detector system is located 300m downstream from the primary target, which aims to study the neutrino beam properties at the time of production.*

background of the primary 12GeV/c protons. This enables us to extrapolate the neutrino flux from the near site to the far site in the $E_\nu \geq$ 1GeV region within an accuracy of $\sim \pm 10\%$.[1]

Fig. 2 shows a record of the protons on target, on which some memorial dates for the experiment are also recorded. After the success of the fast extraction of protons for the experiment on February 3^{rd} 1999, neutrino beam commissioning started on March 4^{th}. After engineering runs to study neutrino beam operations in April through May, stable data taking began in June, 1999. At that time we employed an aluminum target with $2cm\phi$ and a horn current of 200 kA. The typical proton intensity was 4.5×10^{12} *protons-per-pulse*. On June 19^{th}, we observed the first K2K signal at SK. It was the first achievement to detect an accelerator-produced neutrino at a distance of hundreds of *km*. [6)]

---

[1] For an energy lower than 1GeV, we employ an empirical pion production model, [5)] which reproduces the pion monitor measurements very well.

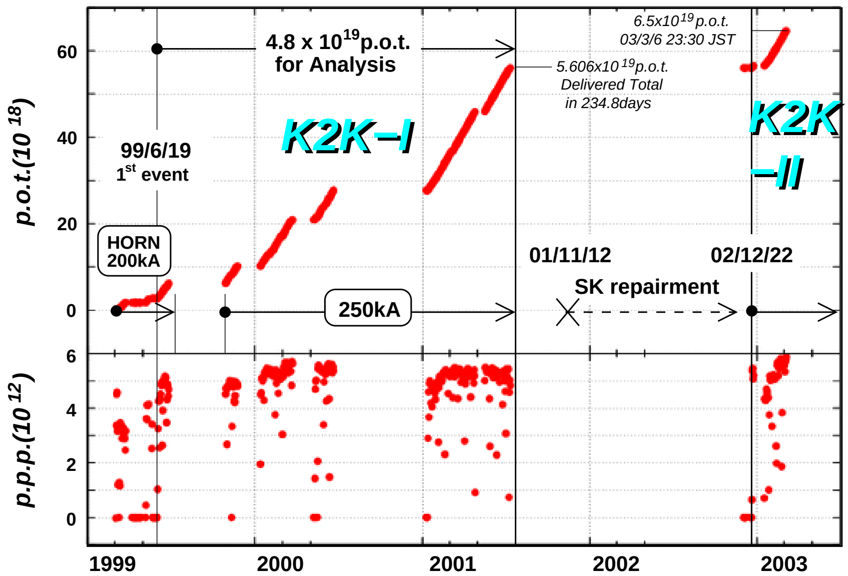

Figure 2: *Accumulated protons on target (upper) and protons per pulse at the target (lower) as function of the date from 1999 to 2003.*

After the summer shutdown, continuous data taking began again in November, with an aluminum target of $3cm\phi$ and a horn current of 250 kA. The typical proton intensity was enhanced to $5{\sim}6\times10^{12}$ *ppp*. After the upgrade, we successfully took data during November 1999 to June 2000, and January to July 2001. The accumulated number of protons on the target from the start of the experiment was 5.606×10^{19} in total. Among them, we used data with stable beam operation after June, 1999, for an analysis, which corresponds to 4.8×10^{19} *pot*. All of the results presented in this talk are based on these K2K-I data.

On November 12^{th} 2001, a severe accident broke out in SK: Due to a chain reaction of shock waves, caused by a sudden improsion of one PMT at the bottom, we lost about 60% of the 11,140 PMTs within a few seconds. Owing to a very quick decision that we try to resume the experiment within one year by rearranging the remaining and spare PMTs at half density,[2] [7)] and

[2]In the relevant energy region for atmospheric neutrinos, proton decays and K2K, it is expected that the difference in the SK configurations will cause no changes to the quality of the experiments.

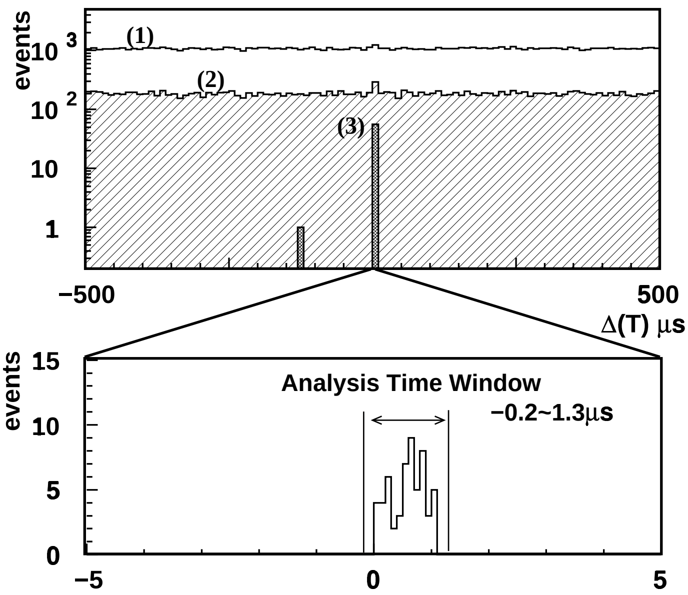

Figure 3: ΔT *($\equiv T_{SK} - T_{KEK} - T_{T.O.F.}$) distributions at each reduction stage at SK in ± 500μsec time window (upper) (1) high-energy trigger condition (2) no decay electron event (3) no activity in the outer detector (fully-contained, FC) and the vertex is in the fiducial volume (FV). ± 5μsec time window for FCFV events (lower).*

also owing to very great efforts to achieve that, SK started data taking again on December 22^{nd}, 2002. The K2K experiment also resumed from that day, and is accumulating data now. We call the data-taking period after the repair as K2K-II.

The GPS system is used [8)] to look for events at SK, which synchronizes to the KEK PS beam pulses. Fig. 3 shows the $\Delta T \equiv T_{SK} - T_{KEK} - T_{T.O.F.}$ distributions at each reduction stage for all K2K-I data. After the final requirements that the event is fully-contained in inner detector (FC) and the neutrino interaction vertex is inside of the 22.5kt fiducial volume (FV), we admit a very clear peak, which coincides to the KEK beam pulse of 1.1μsec width. Inside of an 1.5μsec analysis timing window, which takes the resolution of the ΔT measurement ($<$ 200 nsec) into account, we have observed 56 events in total. The atmospheric neutrino background expected for the timing window is only $\sim 10^{-3}$ events. The arrival times of the events are consistent with a Poisson distributed distribution with regards to the integrated protons on target. Among the FCFV events, 32 events are single-ring (1R) events, and 30 of the 1R events are muon-like events, which are identified by using Cherenkov ring

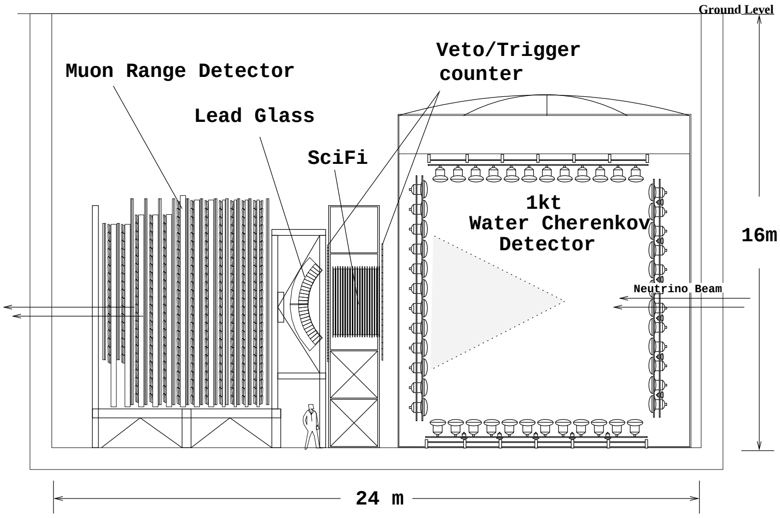

Figure 4: *K2K near detector system, 1kt (right) and FGD (left, composite of SciFi, LG, and MRD). All setups are in a 24mφ - 16m deep well-like hall, so that the neutrino beam, being tilted by about -1° towards the direction of Kamioka, will pass through the center of the detectors.*

image pattern recognition. [9] For the 1Rμ-like events, we can reconstruct the incoming neutrino energy from the muon momentum and angle by assuming a charged-current quasi-elastic interaction, $\nu_\mu + n \to \mu + P$:

$$E_\nu^{\rm rec} = \frac{m_N E_\mu - m_\mu^2/2}{m_N - E_\mu + P_\mu \cos\theta_\mu}, \tag{1}$$

omitting the Fermi momentum and the nuclear potential. We will use the $E_\nu^{\rm rec}$ to see the distortion on the neutrino spectrum shape.

3 Reconstruction of the Neutrino Spectrum by Near Detectors

The K2K experiment employs a near-detector system located 300m downstream from the primary target. Fig. 4 shows a schematic view of the near-detector system. It is composed of two independent detectors: a 1 kiloton SK-like water Cherenkov detector (*1kt*) and a fine-grained detector (FGD). They provide a unique probe for detailed studies on the neutrino-nucleus (H_2O) interactions around E_ν in a few GeV region, which is not yet well understood. [10] We will reconstruct the neutrino energy spectrum at the time of production by analyzing the momentum and angular distributions of muons observed in these two detectors. This is one of the very necessary inputs for oscillation analysis.

3.1 Water Cherenkov detector (*1kt*)

1kt is a miniature of SK with a 1/50 volume, whose data can be directly compared with the SK ones by using the same type of detector and by common analysis procedures. Inside of a 8.6$m\phi$-8.6m height cylinder, 680 of 20" PMTs are arranged in the same 70cm lynning as the SK. The inner volume is 496 tons of purified water, where the event rate in the full volume is 0.2 event per spill. To choose a single interaction per spill, a flash-ADC records the analog sum of all PMTs. The interaction vertex reconstruction, Cherenkov ring counting, and μ-like / e-like ring identification of each ring are performed by the same methods as are employed in the SK. [9] For the K2K spectrum analysis, (1) FCFV-1Rμ-like samples are chosen based on the following selection criteria:

- Events with a >1000$p.e.$ ($\sim$ 100 MeV) single peak in the Flash-ADC (FADC) are chosen. It is used to extract a single interaction in a spill.
- Events with the reconstructed vertex is inside of a cylindrical volume along the beam, $-2m < z < 0m$, $r < 2m$ with a fiducial volume mass=25t (FV events). By these two cuts, the efficiency for those events, which have an interaction vertex in the fiducial volume, is *eff*=75%.
- The total light yield of all PMTs should be in the range of 1000$\sim$20000$p.e.$.
- The maximum response of the inner PMTs is less than 200 $p.e.$. It is used to extract fully contained (FC) events, with it's track endpoint inside of the inner detector (FCFV/Fid.all=75%).
- At last, events with a μ-like single ring pattern are chosen (FCFV1Rμ-like/FCFV=47%).

The characteristics of these events are good sensitivity to the large scattering angle, whereas the sensitivity is limited to the low muon momentum region (p_μ <1 GeV) due to the requirement of the 4^{th} (FC) condition. It is to be noted that in our relevant energy region a recoil proton track is usually not seen (Cherenkov threshold is $p_{thr.}$ $\sim$1.1 GeV/c), and the CCQE interaction is identified as a single ring μ-like event. For the absolute event rate, the measurement has a 5% systematic error, of which the largest contribution comes from the vertex reconstruction uncertainty. For the spectrum measurement, the largest systematic error is an uncertainty on the energy scale. It is known to be within $^{+2}_{-3}$ %, confirmed with both cosmic-ray muons and beam-induced π^0 analysis.

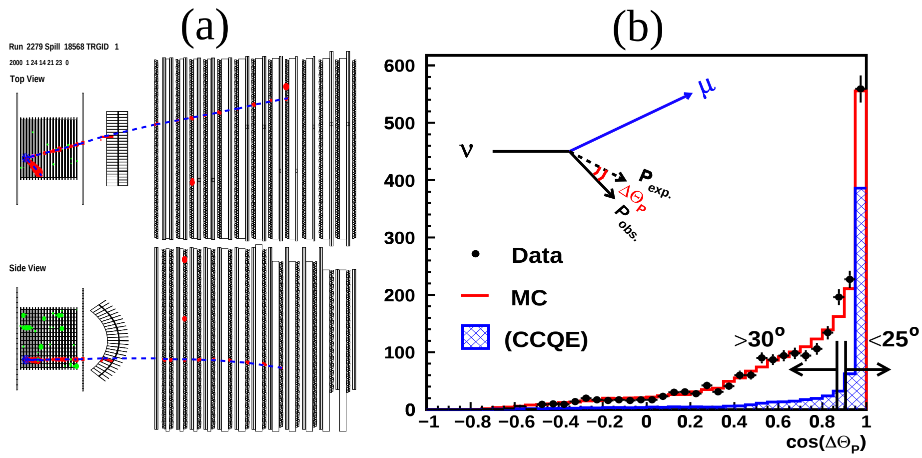

Figure 5: *(a) Typical FGD two track events with an vertex in the SciFi. Track-associated hits are represented by red circles with their size proportional to the number of pixels in the hits. (b)* $cos(\Delta\theta_P)$ *distribution for two-track samples. It is used to distinguish CCQE / non-QE enhanced samples.*

3.2 Fine-Grained Detector (FGD)

FGD aims to measure neutrino interactions precisely by using a tracking-type device. It consists of a scintillating fiber tracker (SciFi), plastic scintillator veto/trigger counters surrounding the SciFi, an electromagnetic calorimeter of 600 lead glass blocks (LG), and a muon range detector (MRD). The SciFi tracker [11] has a $2.6m\times2.6m\times1.7m$ rectangular shape. It is composed of 19 layers of $6cm$-thick water containers, sandwiched with $20\times(yy\text{-}xx)$ layers of $700\mu m\phi$ scintillating fibers. The full weight of the sensitive volume is $8.6t$. All of the fibers are bundled and attached to 24 image intensifier tubes. CCD pixel images are analyzed for hit and track reconstruction. The track finding efficiency [12] is 70% for a track passing through three layers of scintillating fiber and close to 100% for more than 5 layers. Three layers is the minimum track length required in this analysis. MRD [13] measures the momentum of a muon coming out from the SciFi by it's range. It is a sandwich of 12 iron plates $(10cm\times4 + 20cm\times8)$ with drift chambers, covering a $7.6m\times7.6m$ transverse area of the beam. The total mass is 915 tons and events contained in MRD are very important to monitor the neutrino beam stability for the rate and for the profile. For neutrino spectrum reconstruction, we choose SciFi-MRD events with the following criteria:

- A vertex with track(s) with a length $\geq$ 3 SciFi layers is reconstructed.

Table 1: *Statistics of the near-detector events for each category used in the spectrum analysis. Details of the event selection are given in the main text.*

		$pot(\times 10^{19})^{\dagger}$	# Events	$dof.^{\ddagger}$
***1kt* FCFV1Rμ**	**(1)**	3.213	22,476	79
SciFi-MRD		3.970	8,393	
Single Track	**(2)**		5,963	44
2-track $\Delta\theta_P \leq 25°$	**(3)**		764	40
2-track $\Delta\theta_P > 30°$	**(4)**		1,288	40

† *pot* value corresponding to the part of data used for the spectrum analysis.
‡ Number of points on the (p_μ, θ_μ) plane used in the spectrum fit.

The fiducial volume is defined as a rectangle with Δx and $\Delta y \leq 1.1m$, covering the 1^{st} to 17^{th} water containers (fiducial mass= 5.9 t).

- A SciFi track should match to a hit of the downstream veto/trigger counters: This guarantees that the interaction is in a beam spill.
- The track also should match to a LG cluster, and to a MRD track and/or hit cells.

The last condition guarantees that the track passes the LG cells, and is thus a minimum-ionizing muon. At the same time, the cut limits the p_μ sensitivity in the range greater than $\sim$ 500MeV/c. With all of these cuts, the *net* efficiency in the fiducial volume is ~45% for the CCQE interactions and ~31% for the CC-*inclusive* interactions. The momentum of the primary muon track is measured by its range with an accuracy of 2.7%, which is a linear sum of the weight accuracy and a dE/dx uncertainty of the iron. Fig. 5(a) shows a typical FGD event with a secondary track, probably a scattered proton. It is thus a candidate of a CCQE interaction, $\nu_\mu + n \to \mu + P$. For two-track events, a kinematic variable, $\Delta\theta_P$, is defined to enhance the fraction of CCQE and non-QE interactions: Assuming a QE interaction (omitting the effect from Fermi motion), the direction of the scattered proton can be calculated from the muon momentum. We define $\Delta\theta_P$ as the difference between the observed direction of the second track and that of the expectation. Fig. 5(b) shows the $cos(\Delta\theta_P)$ distribution. CCQE events, shown by a hatched histogram, concentrate around $cos(\Delta\theta_P) = 1$, *i.e.* $\Delta\theta_P = 0$.[3] We select a CCQE enhanced sample by requiring $\Delta\theta_P$ within 25 degrees, and non-QE enhanced samples by $\Delta\theta_P$ more than 30 degrees, respectively. In the CCQE enhanced sample, 62% of the events are

[3]Proton re-scattering inside of Oxygen nuclei is taken into account. [14)]

to be QE events. In the non-QE enhanced sample, 82% of events come from interactions other than CCQE. The SciFi events are divided into three event categories: (2) 1-track, (3) 2-track CCQE enhanced, and (4) 2-track non-QE enhanced samples, respectively. The observed number of events for each event category is summarized in Table 1.

3.3 Neutrino Spectrum Reconstruction

The 2-dimensional distributions of the muon momentum versus angle with respect to the beam direction of four event categories, *i.e.* (1) the *1kt* event samples and the three SciFi event samples, (2)$\sim$(4), are used to reconstruct the neutrino spectrum at the time of production. A χ^2-fitting method is used to compare these data against the MC expectation. The neutrino spectrum is divided into 8 energy bins, as defined in Table 2. During the fit, the flux in each energy bin is re-weighted relative to the values in the beam MC. These weights are normalized so that the $E_\nu = 1.0-1.5$ GeV bin is unity, and an overall normalization is introduced as a free parameter. In addition, a parameter, R_{nqe}, is used to re-weight the ratio between the QE and non-QE cross section relative to the MC simulation for the entire E_ν region. It is to be noted that R_{nqe} is strongly constrained by the ratio between the number of events in category (3) and that in category (4). The systematic uncertainties of each detector, *i.e.* the energy scales, the track finding efficiencies, and the detector thresholds, are incorporated as fitting parameters. The spectrum measurement by the pion monitor is also used as a constraint on the flux re-weighting factors.

The best-fit results of the flux re-weighting factors, Φ_{ND}, are shown in Table 2. All of the parameters, including the detector systematics, are found to lie within their expected errors. The χ^2 is 227.2/197 d.o.f.. The muon momentum and angular distributions of each event category are overlaid with the re-weighted MC in Fig. 6. As can be seen, the fit result agrees well with the data. The errors of the fit are provided in the form of an error matrix, and correlations between the parameters are taken into account in the following oscillation analysis. The diagonal elements in the matrix, $\Delta(\Phi_{ND})$ are also given in Table 2.

3.4 Neutrino Interaction Models

The uncertainty due to neutrino interaction models is studied separately. Our MC treats neutrino-nucleus interactions through the following four branches: [15] CC Quasi elastic scattering (CCQE), CC 1π production through baryon resonances (CC1π), Coherent π production, and deep inelastic scattering:

- In CCQE scattering, the axial vector mass in the dipole formula is set to a central value of 1.1 GeV/c^2, and is varied by $\pm10\%$.

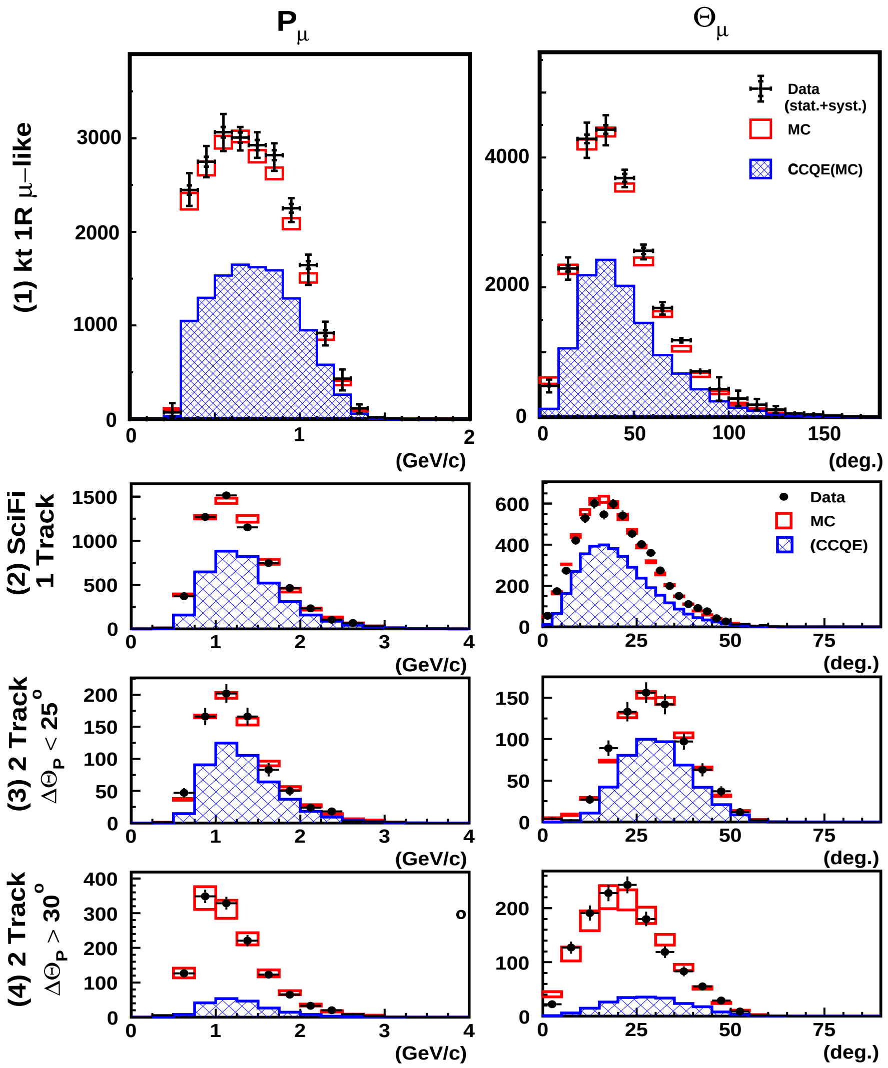

Figure 6: *Muon momentum (left) and angle (right) distributions for each event category: (1) 1kt FCFV single-ring μ-like events, (2) SciFi single-track events, (3) 2-track QE enhanced events, and (4)2-track non-QE enhanced events. The crosses are data and the boxes are MC with the best fit parameters. The errors on the MC distributions correspond to the uncertainties of each flux bin and R(nonQE/QE). The hatched histograms show the CCQE contributions.*

Table 2: *Central values of the flux re-weighting parameters for the spectrum fit at the near detectors ($\Phi_{\rm ND}$) and the percentage size of the energy dependent systematic errors on the re-weighting parameters ($\Delta(\Phi_{\rm ND})$), F/N ratio, and reconstruction efficiency for 1Rμ events at SK ($\epsilon_{\rm SK}$). $\Phi_{\rm ND}$s are given relative to the 1.0−1.5 GeV energy bin.*

E_ν (GeV)	$\Phi_{\rm ND}$	$\Delta(\Phi_{\rm ND})$	Δ(F/N)†	$\Delta(\epsilon_{\rm SK})^\ddagger$
0−0.5	1.31	±49	±2.6	±8.7
0.5−0.75	1.02	±12	±4.3	±4.3
0.75−1.0	1.01	±9.1	±4.3	±4.3
1.0−1.5	≡ 1.00	—	±6.5	±8.9
1.5−2.0	0.95	±7.1	±10	±10
2.0−2.5	0.96	±8.4	±11	±9.8
2.5−3.0	1.18	±19	±12	±9.9
3.0−	1.07	±20	±12	±9.9

† Errors are quoted from the pion monitor measurement in >1 GeV, and from the uncertainties in hadron production models in <1 GeV, respectively.
‡ The error on the particle identification dominates in <0.5 GeV, and the error on ring counting dominates in >1 GeV, respectively.

- The axial mass for CC1π is set to a central value of 1.2 GeV/c^2, and is varied by ±20%. [16]
- For coherent pion production, the Rein and Sehgal model [17] and a model by Marteau [18] are compared.
- For deep inelastic scattering, GRV94 [19] and the corrected structure function by Bodek and Yang [20] are both studied.

For an oscillation analysis, the Marteau model and Bodek and Yang structure functions are employed. Varying the choice of models causes the fitted value of R_{nqe} (= 0.93) to change by $\sim$ 20%. In order to account for this, an additional systematic error of ±20% on R_{nqe} is added by hand. It is found that the choice of models does not affect the Φ_{ND} values, themselves, beyond the size of the fitted errors. Also, it is to be noted that the effects of the model difference on the oscillation analysis is found to be negligible, because of a cancellation between the near cite and the far cite measurements.

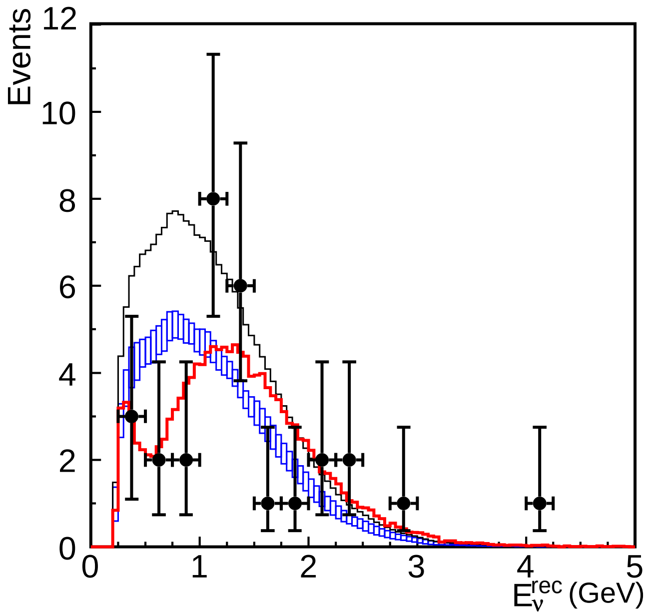

Figure 7: *Reconstructed E_ν distribution for the $1R\mu$ sample. The points with error bars are data. The box histogram is the expected spectrum without oscillations, where the height of the box is the systematic error. The thick-solid line is the best-fit spectrum. These histograms are normalized by the number of observed events, 29. In addition, the thin-solid line shows the expectation with no oscillations normalized to the expected number of events, 44.*

4 Oscillation Analysis

A two-flavor neutrino oscillation analysis with ν_μ disappearance is performed by the maximum-likelihood method. In the analysis, both the number of FCFV events (56) and the energy spectrum shape for $1R\mu$ events (29) are used.[4] The likelihood is defined as

$$\mathcal{L} = \mathcal{L}_{norm} \times \mathcal{L}_{shape}, \tag{2}$$

where the normalization term, $\mathcal{L}_{norm}(N_{obs}, N_{exp})$, is the Poisson probability to observe N_{obs} events when the expected number of events is $N_{exp}(\Delta m^2, \sin^2 2\theta, f)$. Here, the symbol f represents a set of parameters constrained by the systematic errors. They consist of the re-weighted neutrino spectrum measured at the

[4]Data taken in June 1999 are discarded for $\mathcal{L}_{shape}$, because the spectrum shape was different from that for the rest of the running period due to the different horn configuration. The data correspond to 6.5% of the total *pot*.

near detectors (Φ_{ND}), the F/N ratio, the reconstruction efficiency (ϵ_{SK}) of SK for $1R\mu$ events, the re-weighting factor for the QE/non-QE ratio (R_{nqe}), the SK energy scale (3% [9]) and the overall normalization. Note that the errors on the first 3 items depend on the energy and have correlations between each energy bin. The diagonal parts of their error matrices are summarized in Table 2. Since the *1kt* has the same kind of detector as SK, most of the systematic uncertainties on the measurement are expected to be canceled to each other. The expected number of FCFV events, N_{exp}, at SK without oscillation with an overall normalization measured by the *1kt* is estimated to be $80.1^{+6.2}_{-5.4}$, which is to be compared to $N_{obs} = 56$. The major contributions to the errors come from the uncertainties in the F/N ratio ($^{+4.9\%}_{-5.0\%}$) and the normalization (5.0%). The latter is dominated by uncertainties of the fiducial volumes due to vertex reconstruction errors at both the *1kt* and SK. On the other hand, the shape term,

$$\mathcal{L}_{shape} = \prod_{i=1}^{N_{1R\mu}} P(E_i; \Delta m^2, \sin^2 2\theta, f), \tag{3}$$

is a product of the probability for each $1R\mu$ event to be observed at $E_\nu^{\rm rec} = E_i$, where P is the normalized $E_\nu^{\rm rec}$ distribution, estimated by MC, and $N_{1R\mu}$ is the number of $1R\mu$ events. The number of $1R\mu$ events observed (excluding the data of June 1999) is 29, and the corresponding number of $1R\mu$ events expected from MC in the case of no oscillation is 44. The likelihood is calculated at each point in the Δm^2 and $\sin^2 2\theta$ space to search for the point where the likelihood is maximized.[5] As a result, the best-fit point is found to be at $(\sin^2 2\theta, \Delta m^2){=}(1.0, 2.8{\times}10^{-3}\ {\rm eV}^2)$. [6] At the best-fit point the predicted total number of FCFV events is 54.2, which agrees with the observation (56) within the statistical error. The observed $E_\nu^{\rm rec}$ distribution of the $1R\mu$ sample is shown in Fig. 7 together with the expected distributions for the best-fit oscillation parameters, and the expectation without oscillations. The best-fit spectrum shape agrees with the observations. Fig. 8(a) shows the allowed regions of oscillation parameters, evaluated by calculating the likelihood ratio of each point to the best-fit point. The 90% C.L. contour crosses the $\sin^2 2\theta = 1$ axis at $\Delta m^2{=}1.5$ and $3.9{\times}10^{-3}\ {\rm eV}^2$. Fig. 8(b) shows a $-ln\mathcal{L}$ behavior at $\sin^2 2\theta = 1$ slice, which shows that the Δm^2 preferred by the total flux suppression and the energy distortions alone agree well. The probability that the observations are due to a statistical fluctuation instead of neutrino oscillation is calculated to be 0.7%. When only normalization (shape) information is used, the probabilities are estimated to be 1.3% (16%), respectively.

---

[5] We treat the systemtic parameters, f, as fitting parameters, with an additional constraint term in the likelihood.

[6] $(1.03, 2.8 \times 10^{-3}\ {\rm eV}^2)$ if the unphysical region is taken into account.

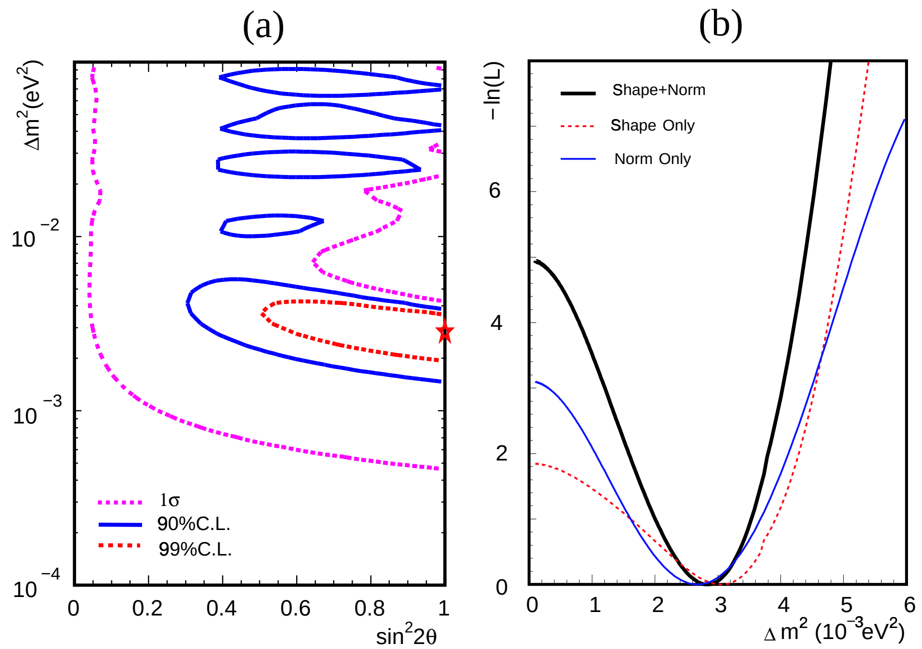

Figure 8: *(a) Allowed regions of oscillation parameters. Dashed, solid and dot-dashed lines are 68.4%, 90% and 99% C.L. contours, respectively. The best fit point is indicated by a star. (b) Behavior of negative log likelihood along* $sin^2 2\theta=1$*. Analysis results of number of event only (thin-solid) and shape only (dashed) are also given, which suggest mutually consistent* Δm^2 *values.*

5 Conclusion

The K2K experiment has collected approximately one-half of its planned 10^{20} protons on target in K2K-I. During the period of running, we have collected 56 FCFV events at SK, which should be compared to the expectation, $80.1^{+6.2}_{-5.4}$. 29 1Rμ-like events are further used to study the spectrum distortion, and both the number of FCFV events and the energy spectrum are found to be consistent with neutrino oscillation. A combined likelihood analysis gives ($\sin^2 2\theta$, Δm^2)=($1.0, 2.8\times10^{-3}$ eV^2) as the best-fit values. The 90% C.L. contour crosses $\Delta m^2 = 1.5 \sim 3.9 \times 10^{-3}$eV^2 at $sin^2 2\theta$=1.0, which are consistent with the ones suggested by atmospheric neutrinos. The probability that the measurements at SK can be explained by statistical fluctuation is found to be less than 1%. After the recovery from the accident at SK, we started a new phase of K2K-II, to provide sufficient statistics for a further study on neutrino oscillation.

References

1. Outline of the present talk is based on the references: M.H. Ahn *et al.* [K2K collaboration] Phys. Rev. Lett. bf 90, 041801 (2003). See also S.H. Ahn *et al.* [K2K collaboration] Phys. Lett. **B511**, 178 (2001).
2. Y. Fukuda *et al.* [Super-Kamiokande collaboration], Phys. Rev. Lett. **81**, 1562 (1998); L. Sulak, *this conference.*
3. H. Noumi *et al.*, Nucl. Instrum. Meth. **A 398**, 399 (1997).
4. T. Maruyama, Ph. D thesis, Tohoku Univ. (2000).
5. Y. Cho *et al.* Phys. Rev. **D 4**, 1967 (1971).
6. http://neutrino.kek.jp/news/990628.1stSK/index.html
7. http://neutrino.kek.jp/news/2001.11.12.html
8. H.G. Berns and R.J. Wilkes, IEEE Nucl. Sci. **47**, 340 (2000).
9. Y. Fukuda *et al.* [SK collaboration], Phys. Lett. **B433**, 9 (1998).
10. T. Ishida, in: Proc. The First International Workshop on Neutrino-Nucleus Interactions in the Few GeV Region (NuInt01), (ed. J.G. Morfin, M. Sakuda and Y. Suzuki, KEK, December 2001), Nucl. Phys. **B** (*Proc. Suppl.*) **112**, 132 (2002).
11. A. Suzuki *et al.*, Nucl. Instr. and Meth. **A 453**, 165 (2000).
12. B.J. Kim *et al*, Nucl. Instr. and Meth. **A497**, 450 (2003).
13. T. Ishii *et al.*, Nucl. Instr. and Meth. **A 482**, 244 (2002).
14. C.W. Walter, Nucl. Phys. **B** (*Proc. Suppl.*) **112**, 140 (2002).
15. Y. Hayato, Nucl. Phys. **B** (*Proc. Suppl.*) **112**, 171 (2002).
16. V. Bernard, L. Elouadrhiri, and U.G. Meissner, J. Phys. **G28**, R1 (2002).
17. D. Rein and L.M. Sehgal, Nucl. Phys. **B223**, 29 (1983).
18. J. Marteau et al., Nucl. Instrum. Meth. **A451**, 76 (2000).
19. M. Gluck, E. Reya, and A. Vogt, Z. Phys. **C67**, 433 (1995).
20. A. Bodek and U.-K. Yang, Nucl. Phys. **B** (*Proc. Suppl.*) **112**, 70 (2002).